Path integral Monte Carlo benchmarks for two-dimensional quantum dots

Ilkka Kylänpää* and Esa Räsänen
Laboratory of Physics, Tampere University of Technology, P.O. Box 692, FI-33101 Tampere, Finland
(Dated: October 30, 2017)

We report numerically accurate path integral Monte Carlo results for harmonically confined two-dimensional quantum dots containing up to $N = 60$ interacting electrons. The finite temperature values are extrapolated to zero Kelvin and zero time step in order to provide precise upper-bound energies. The ground-state energies are compared against coupled-cluster and diffusion Monte Carlo results available in the literature for $N \leq 20$. We also provide Padé fits for the energies as a function of N for different strengths of the confining potential. The fits deviate less than 0.25% from the path integral Monte Carlo data. Overall, our upper bound estimates for the ground-state energies have lower values than previous diffusion Monte Carlo benchmarks due to the accurate nodal surface in our simulations. Hence, our results set a new numerical benchmark for two-dimensional (spin-unpolarized) quantum dots up to a large number of electrons.

I. INTRODUCTION

Nowadays, quantum dot (QD) technology is an integral part in developing novel solid state devices. These so-called artificial atoms can be utilized individually, as clusters or as periodic arrays, which results in a number of possible applications.[1–4] Theoretical and computational approaches are, however, needed for better understanding of the behavior of electrons in quantum dots, and in making new predictions.[5–22]

There is a large variety of theoretical and computational approaches available for QD simulations, but commonly their applicability is limited to certain confinement strengths or to only a few electrons. The limitations generally arise from the description of electron-electron correlations, which are more pronounced with weaker confinement strengths, and in the scaling of the method as a function of the number of electrons.

Previous numerical benchmarks for QDs beyond the few-electron regime, i.e., for $N \gtrsim 10$, have been obtained by using coupled-cluster[5,6] (CC) and diffusion Monte Carlo[6] (DMC) methods. The CC method has employed singles and doubles (CCSD), as well as singles, doubles and triples denoted by CCSD(T). In the CC method, the quality of the basis has a substantial effect on the accuracy[5] and, in general, the method is best applicable to closed-shell systems. In the previous DMC simulations, the nodal structure was adopted from density-functional theory calculations using the local-density approximation (DFT-LDA).[6]

In this study we provide benchmark ground-state energies for QDs using the path integral Monte Carlo (PIMC) method.[23–26] PIMC is a finite-temperature approach with exact particle-particle correlations. As a basis-free method it avoids the challenges in, e.g., the basis-dependent CC methods. However, similarly to most quantum Monte Carlo (QMC) methods, the description of the exchange interaction is challenging at low temperatures. In this work this challenge is dealt with by the so-called free-particle nodes.[27] In order to ensure upper bound estimates, our total energies are extrapolated to zero time step. Moreover, we extrapolate our finite-temperature PIMC results to zero Kelvin, which enables proper comparison to the most accurate QD energies in the literature.

II. MODEL AND METHOD

In atomic units with energies in Hartrees ($E_{\rm H}$) our model Hamiltonian for the harmonic QD reads

$$H = \sum_{i=1}^{N} \left[-\frac{1}{2m_e}\nabla_i^2 + \frac{1}{2} m_e \omega^2 r_i^2 \right] + \sum_{i<j} \frac{1}{\varepsilon |\mathbf{r}_i - \mathbf{r}_j|}. \quad (1)$$

Here we focus on GaAs QDs for which we adopt the same parameters and confinement strengths as those in Refs. 5 and 6, i.e., $m_e = 0.067$, $\varepsilon = 12.4$, and $\hbar\omega = 3.3200$, 5.9286, and 11.857 meV. The energies and lengths convert to effective atomic units as $E_{\rm H}^{\rm eff} = \frac{\varepsilon^2}{m_e} E_{\rm H}$ and $r^{\rm eff} = \frac{m_e}{\varepsilon} r$. In effective atomic units the confinement strengths are $\hbar\omega = 0.28$, 0.5, and $1.0 E_{\rm H}^{\rm eff}$, which we use from now on. We point out that we focus solely on spin-unpolarized systems, i.e., $N_\uparrow = N_\downarrow = N/2$.

Path integrals are based on the Feynman formulation of quantum statistical mechanics,[28] which enables the study of quantum many-body effects at finite temperature. Combined with Metropolis Monte Carlo sampling of the configuration space,[29] the method is referred to as PIMC. It can be efficiently used to accurately account for both finite temperature and correlation effects. Improved sampling is obtained by using multilevel bisection moves.[30]

Fermi statistics is employed by restricted path integral formalism,[27] in which the density matrix is given as

$$\rho_F(R_\beta, R_\star; \beta) = \int dR_0 \rho_F(R_0, R_\star; 0) \int_{\gamma: R_0 \to R_\beta}^{\gamma \subset \Upsilon_\beta(R_\star)} dR_t e^{-\mathcal{S}[R_t]},$$

where $\beta = 1/k_{\rm B}T$, F refers to the Fermion density matrix, S is the action, $R_\star$ is the so-called reference point, and Υ_β is a region in "space-time" that specifies the boundary conditions for the Bloch equation. Here, we use the nodes of the free-particle density matrix[27] to determine the boundary conditions, and we demonstrate that these nodes can be considered to be of high accuracy especially for the harmonic QDs under consideration. For the energetics we use the Herman type virial estimator.[31]

III. RESULTS AND DISCUSSION

For the confinement strengths $\hbar\omega = 0.28$, 0.5, and $1.0E_{\rm H}^{\rm eff}$, and electron numbers $N = 6$, 12, 20, 40, and 60 we provide accurate PIMC data at $T/T_{\rm F} = 0.025$ in addition to the extrapolated PIMC values at zero Kelvin. The error estimates in this work are given as 1-σ statistical error of the mean. For two electrons with $\omega = 1.0E_{\rm H}^{\rm eff}$ the harmonic dot can be exactly solved yielding the total energy of $3.0E_{\rm H}^{\rm eff}$.[32] With our PIMC implementation we obtain a value of $2.99994(9)E_{\rm H}^{\rm eff}$ at $T/T_{\rm F} = 0.005$ in good agreement with the exact result. However, let us first elaborate what is needed in order to obtain the benchmark PIMC results presented in this article.

PIMC method is the more efficient the higher the temperature, which is naturally advantageous in dealing with temperature effects. Here, however, we focus on low temperatures in accordance with most experimental and theoretical works on QDs. We consider $T = 0$ in particular, which requires extrapolation based on several temperatures. For $N \leq 20$ we use four temperatures ($T/T_{\rm F} = 0.0125$, 0.025, 0.05, and 0.1) for the extrapolation. We use additional fifth temperature at $T/T_{\rm F} = 0.008$ for a few cases to validate the agreement with our fit. For the $N = 40$ case we use five temperatures: $T/T_{\rm F} = 0.0125$, 0.017, 0.025, 0.05, and 0.1. The temperature effects are considered with our second smallest time-step, i.e., $\tau = 0.019531E_{\rm F}^{-1}$.

With the increasing number of electrons it is desirable to use as high temperature as possible, and thus, for the $N = 60$ case we performed simulations only at a temperature relatively close to the ground state, i.e., at $T/T_{\rm F} = 0.025$. In this case, we obtain the zero Kelvin value by estimating the temperature effects from our $N \leq 40$ simulations: We optimized the coefficients α, a, and b in $N^{-\alpha}\Delta E = aN + b$, and used that expression to estimate ΔE for $N = 60$. In Table I we show the values for ΔE that can be used in the extrapolation to zero from $T/T_{\rm F} = 0.025$. These values can be used in estimating the temperature effects by interpolation or extrapolation in future PIMC studies also. This will reduce the computational time, since simulations only at $T/T_{\rm F} = 0.025$ are needed.

TABLE I: Estimation of the temperature effects ΔE on the total energy at $T/T_{\rm F} = 0.025$ with one sigma statistical error estimate in the parenthesis. Notice that $E(T = 0) \approx E(T/T_{\rm F} = 0.025) + \Delta E$. Energies are given in effective atomic units.

	$\hbar\omega$	$\Delta E_{\rm tot}$
$N = 6$	0.28	$-0.0053(3)$
	0.50	$-0.0083(4)$
	1.00	$-0.0158(7)$
$N = 12$	0.28	$-0.0358(12)$
	0.50	$-0.054(2)$
	1.00	$-0.096(5)$
$N = 20$	0.28	$-0.153(5)$
	0.50	$-0.212(9)$
	1.00	$-0.33(2)$
$N = 40$	0.28	$-0.168(6)$
	0.50	$-0.30(6)$
	1.00	$-0.8(1)$
$N = 60$	0.28	$-0.21(5)$
	0.50	$-0.41(6)$
	1.00	$-1.3(2)$

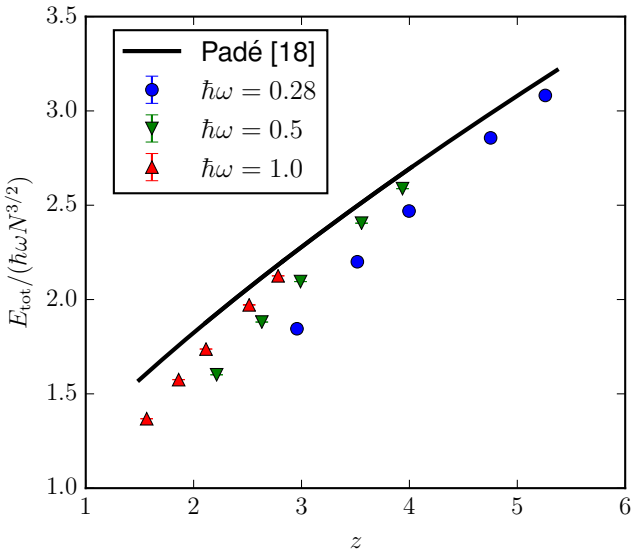

FIG. 1: Scaling relation of the ground state energy from Ref. 18 (solid line) and path integral Monte Carlo data with three different confinement strenghts (symbols). Large-N values tend towards the Padé form of the scaling function as expected.

In order to obtain upper bound estimates we have extrapolated our PIMC data to zero time-step at $T/T_{\rm F} = 0.025$ for all the cases. We have used six different time-steps, $\tau \approx 0.0098$, 0.0195, 0.0391, 0.0781, 0.15625, and 0.31250 in units of $E_{\rm F}^{-1}$, and a third-order polynomial fit. The behavior of the total energy as a function of time-step (τ) becomes linear as τ tends to zero. These upper bound values at $T/T_{\rm F} = 0.025$ are then extrapolated to zero Kelvin using the values in Table I.

Next, let us consider the behavior of the ground state energies with respect to the large-N scaling relation given in Ref. 18 in a form of a Padé approximant. It is given as

$$\frac{E_{\rm gs}}{\hbar\omega N^{3/2}} \approx \frac{2}{3} + \frac{0.698z + 1.5z^4 + 2.175z^{5/3}}{1 + 2.149z^{1/3} + 1.5z^{2/3} + 2.175z}, \quad (2)$$

where $z = N^{1/4}\omega^{-1/2}$ in effective atomic units.

In Fig. 1 we present the scaling relation as "Padé" (solid line) and our extrapolated PIMC results (symbols). Clearly, as z is increasing, the PIMC data tend towards the large-N scaling relation. This tendency is pronounced for large confinements, i.e., weaker electron-electron interactions. This expected behavior demonstrates the rather good predictability of the scaling relation for large N.

Despite the general validity of the trend in Fig. 1, there are significant deviations from the Padé curve for, e.g., $z \approx 3.36$

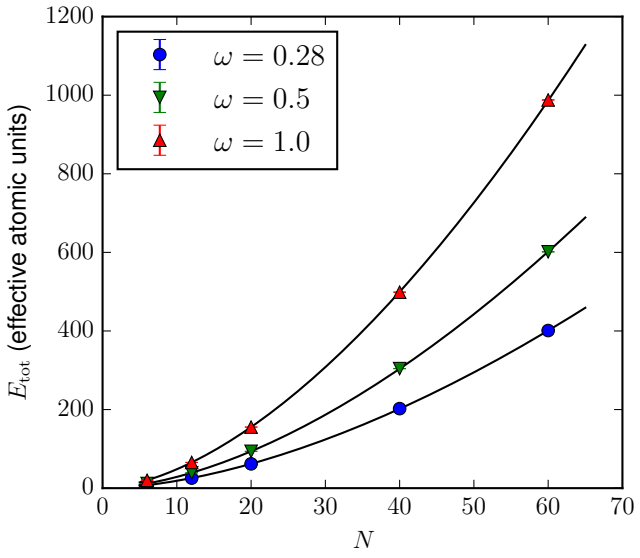

FIG. 2: Modified Padé fits to our PIMC data, see Eq. (3). The fits yield better than 0.24% accuracy with respect to our PIMC data, and on average the discrepancy is less than 0.1%. The PIMC data points correspond to $N = 6$, 12, 20, 40, and 60, and the energy values are shown in Table IV.

and $\omega = 0.28$. However, we can modify the functional form in Eq. (2) to obtain accurate fits for all the PIMC energies. This is achieved through the following form:

$$E_{\rm tot} = \hbar\omega N^{3/2}\left[\frac{2}{3} + \frac{az + 1.5z^4 + 2.175z^{5/3}}{1 + bz^{1/3} + 1.5z^{2/3} + 2.175z}\right], \quad (3)$$

where a and b are two parameters that can be optimized for each confinement strength, respectively, to fit with the PIMC data. In our examples we obtain $a = -5.09904703$ and $b = -4.64163077$ for $\hbar\omega = 0.28$, $a = -4.17789992$ and $b = -3.74168272$ for $\hbar\omega = 0.5$, and $a = -3.2961045$ and $b = -2.88621374$ for $\hbar\omega = 1.0$. These parameters yield better than 0.24% accuracy to our PIMC data, and on average the discrepancy is less than 0.1%. Our PIMC data gives lower upper bound estimates than the DMC results of Ref. 6, which actually deviate from our data on average by 0.20% having the maximum discrepancy of 0.32%. Therefore, our fit should provide even more accurate reference data than the DMC based on DFT-LDA nodal structure. The fits are shown in Fig. 2. We point out that the above procedure, i.e., the PIMC calculation for a few N followed by the two-parameter Padé fit according to Eq. (3), can be repeated for any confinement strength to obtain an accurate trend as a function of N. However, due to the spin-independent scheme used here, we do not account for the fine structure in $E(N)$ resulting from nontrivial spin polarization at certain N according to Hund's rules.

Despite the lack of spin effects we can assess the electrochemical potentials of QDs defined as $\mu(N) = E(N) - E(N-1)$. This is demonstrated in Table II. In general, the values are in a reasonable agreement. Interestingly, the PIMC fit seems to provide "extrapolation" of the CC and DMC values. That is, CC has always either the largest or the smallest value, and DMC value is always in between CC and PIMC result. Nevertheless, we leave further calculations and analyses of chemical potentials to future works, where spin effects should be incorporated.

TABLE II: Electrochemical potential $\mu(N) = E(N) - E(N-1)$ for $\hbar\omega = 0.28$ from our fits (Fig. 2 and Eq. (3)) compared with available values in the literature. The energies are given in effective atomic units.

	CC[6]	DMC[6]	PIMC fit
$E(3) - E(2)$	1.2284	1.2123(1)	1.1612
$E(6) - E(5)$	2.0438	2.0663(1)	2.1166
$E(7) - E(6)$	2.4528	2.4341(1)	2.3921
$E(12) - E(11)$	3.5420	3.5618(1)	3.6025
$E(13) - E(12)$	3.8738	3.8582(1)	3.8213

In Table III we present our PIMC energies at $T/T_{\rm F} = 0.025$. The results include the total energy ($E_{\rm tot}$), kinetic energy ($E_{\rm kin}$), total potential energy ($E_{\rm pot}$), and the electron-electron interaction energy ($E_{\rm ee}$). The contribution of the harmonic confinement is thus $E_{\rm harm} = E_{\rm pot} - E_{\rm ee}$. The energies in Table III have been extrapolated to zero time-step, and therefore, they provide an upper bound estimate for the total energy at this temperature.

By adding the values from Table I to the total energies in Table III we obtain the extrapolated $T = 0$ values. They are shown in Table IV in comparison with other high-accuracy values in the literature. In general, the PIMC energies are slightly lower than those obtained with CC or DMC methods. For $N = 12$ and $\hbar\omega = 0.28$, the CCSD result of Ref. 5 is lower than the PIMC, but the difference is very small, and it should also be noted that the CC is not an upper-bound estimate. Moreover, it is good to point out that the differences between the PIMC and DMC energies cannot be explained by uncertainties in the extrapolations to zero temperature and to zero time-step. Even in the case in which we would expect the smallest effects related to the nodal surface, i.e., $N = 6$ and $\omega = 0.28$, the error from above in the temperature extrapolation can be estimated to be $\epsilon_{T=0} \leq 0.000224 E_{\rm H}^{\rm eff}$, while an upward exaggerated error estimate in the time-step extrapolation would give $\epsilon_{\tau=0} \leq 0.003 E_{\rm H}^{\rm eff}$. Using the maximum values would still give us $\sim 0.0040(2) E_{\rm H}^{\rm eff}$ lower total energy than DMC in the case that is expected to have the smallest discrepancy.

In some cases, there are relatively large discrepancies between the two CC implementations using different basis functions. For CCSD, the results in Ref. 5 are generally more accurate compared against our PIMC values. For the CC in Ref. 6, the addition of triples makes a considerable improvement in the results. Therefore, it would be interesting to obtain CCSD(T) values also for the implementation of Ref. 5. Maybe even an extension to quadrupoles would be advisable, but expectedly this is computationally very demanding, especially for higher N. PIMC does not suffer from basis set dependence, but – on the other hand – very accurate nodal surfaces

are called for in calculations of atoms, molecules, and solids at low temperatures. In the present case of semiconductor QDs, the free particle nodes are sufficient to yield accurate results.

The main advantage of PIMC is the straightforward account of finite temperature and correlations between particles irrespective of the external potential. At its current state-of-the-art it is most feasible in treating model systems and low-Z materials at intermediate to high temperatures, but progress towards high accuracy materials modeling will be possible hopefully already in the near future. As shown here, PIMC is already capable of treating accurately quite large numbers of interacting electrons in finite systems. It should be pointed out that for only a few particles the simulations are rather effortless, although this is dependent on the external potential of the particles. In general, the attractive Coulomb potential is challenging especially for higher Z elements, which stems from the fact that the potential is not bound from below. For model potentials, such as individual quantum dots or arrays of quantum dots of various shapes, these challenges are absent, which make them ideal objects for more path integral studies.

IV. CONCLUSIONS

In this study we produce benchmark energies for two-dimensional harmonic quantum dots up to $N = 60$ electrons with the path integral Monte Carlo method. The finite temperature values are extrapolated to zero Kelvin and zero time-step in order to provide accurate upper-bound energetics. The ground-state energies are compared against coupled-cluster and diffusion Monte Carlo results available in the literature for smaller N. We find that our upper bound estimates for the ground state energies yield lower values than the diffusion Monte Carlo benchmarks. This tendency is pronounced as the confinement strength is increased. However, the deviations between the two Monte Carlo methods remains below 0.32%. The difference arises from the approximate description of the nodal surface in the diffusion Monte Carlo approach. Using comparable nodal surfaces both methods should lead to the same zero Kelvin total energy, which is evident also from, e.g., the simulations of nodeless systems such as the unpolarized $N = 2$ harmonic quantum dot.

We have also introduced a fit in a form of a Padé approximant for the ground state energies as a function of N. The fit yields smaller than 0.25% deviation from the computed total energies, and the validity of the fit is shown for $N = 6 \ldots 60$. It can also be expected that the fit yields reasonable approximations also at larger N. In conclusion, we believe that the present work represents a useful benchmark for further calculations for semiconductor quantum dots with different computational methods.

V. ACKNOWLEDGMENTS

We thank Eva Lindroth and Carl Wesslén for useful discussions. This work has been supported by the Academy of Finland. We acknowledge CSC – IT Center for Science Ltd. and TCSC – Tampere Center for Scientific Computing for the allocation of computational resources.

TABLE III: Energetics from PIMC simulations at $T/T_{\rm F} = 0.025$ with one sigma statistical error estimate in the parenthesis. The PIMC energies have been extrapolated to zero time-step limit in order to provide an upper bound estimate. Energies are given in effective atomic units.

	$\hbar\omega$	$E_{\rm tot}$	$E_{\rm kin}$	$E_{\rm pot}$	$E_{\rm ee}$
	0.28	7.59804(10)	0.94071(9)	6.65734(3)	3.81109(5)
$N = 6$	0.50	11.7742(2)	1.71402(14)	10.06019(6)	5.56412(8)
	1.00	20.1222(4)	3.5628(3)	16.55937(11)	8.66439(13)
	0.28	25.6456(6)	2.2402(6)	23.40544(13)	14.1102(4)
$N = 12$	0.50	39.1413(10)	4.1325(9)	35.0088(3)	20.5842(5)
	1.00	65.585(3)	8.761(2)	56.8236(6)	32.0418(11)
	0.28	61.992(3)	4.304(2)	57.6879(4)	35.5890(12)
$N = 20$	0.50	93.915(4)	8.020(4)	85.8944(7)	51.916(2)
	1.00	155.737(9)	17.194(8)	138.543(2)	80.899(4)
	0.28	202.55(3)	10.42(3)	192.128(4)	121.137(13)
$N = 40$	0.50	304.48(4)	19.57(4)	284.910(5)	176.89(3)
	1.00	499.6(3)	42.6(3)	456.924(12)	276.19(14)
	0.28	401.28(8)	14.92(17)	386.33(14)	247.6(2)
$N = 60$	0.50	601.78(13)	31.3(3)	570.57(15)	359.5(3)
	1.00	988.2(4)	75.1(6)	913.2(3)	558.7(6)

TABLE IV: Total energies from PIMC simulations extrapolated to $T = 0$ in comparison with other methods. The PIMC energies provide an upper bound estimate. Energies are given in effective atomic units with one sigma statistical error estimate in the parenthesis.

	$\hbar\omega$	PIMC	CCSD[5]	CCSD[6]	CCSD(T)[6]	DMC[6]
	0.28	7.5927(2)	7.605555	7.6252	7.6006	7.6001(1)
$N = 6$	0.50	11.7659(4)	11.80093	11.8055	11.7837	11.7888(2)
	1.00	20.1063(8)	20.18818	20.1737	20.1570	20.1597(2)
	0.28	25.6098(13)	25.59384	25.7089	25.6324	25.6356(1)
$N = 12$	0.50	39.088(3)	39.14125	39.2194	39.1516	39.159(1)
	1.00	65.488(5)	65.74107	65.7409	65.6886	65.700(1)
	0.28	61.839(6)	-	62.0664	61.9156	61.922(2)
$N = 20$	0.50	93.703(9)	-	93.9891	93.8558	93.867(3)
	1.00	155.41(2)	-	155.9601	155.8571	155.868(6)
	0.28	202.38(3)	-	-	-	-
$N = 40$	0.50	304.18(8)	-	-	-	-
	1.00	498.8(4)	-	-	-	-
	0.28	401.07(9)	-	-	-	-
$N = 60$	0.50	601.37(14)	-	-	-	-
	1.00	987.9(5)	-	-	-	-

* Electronic address: kylanpaait@ornl.gov; Present address: Materials Science and Technology Division, Oak Ridge National Laboratory, Oak Ridge, Tennessee 37831, USA

[1] G. Moody and S. T. Cundiff, Adv. Phys.: X **2**, 641 (2017).
[2] M. Polini, F. Guinea, M. Lewenstein, H. C. Manoharan, V. Pellegrini, Nat. Nanotechnol. **8**, 625 (2013).
[3] S. M. Reimann and M. Manninen, Rev. Mod. Phys. **74**, 1283 (2002).
[4] R. Hanson, L. P. Kouwenhoven, J. R. Petta, S. Tarucha, L. M. K. Vandersypen, Rev. Mod. Phys. **79**, 1217 (2007).
[5] E. Waltersson, C. J. Wesslén, and E. Lindroth, Phys. Rev. B **87**, 035112 (2013).
[6] M. Pedersen Lohne, G. Hagen, M. Hjorth-Jensen, S. Kvaal, and F. Pederiva, Phys. Rev. B **84**, 115302 (2011).
[7] I. Kylänpää, F. Cavaliere, N. T. Ziani, M. Sassetti, E. Räsänen, Phys. Rev. B **94**, 115417 (2016).
[8] R. Egger, W. Häusler, C. H. Mak, and H. Grabert, Phys. Rev. Lett. **82**, 3320 (1999).
[9] B. Reusch and R. Egger, Europhys. Lett. **64**, 84 (2003).
[10] S. Weiss and R. Egger, Phys. Rev. B **72**, 245301 (2005).

[11] S. A. Chin, Phys. Rev. E **91**, 031301 (2015).
[12] M. Dineykhan and R. G. Nazmitdinov, Phys. Rev. B **55**, 13707 (1997).
[13] M. B. Tavernier, E. Anisimovas, F. M. Peeters, B. Szafran, J. Adamowski, and S. Bednarek, Phys. Rev. B **68**, 205305 (2003).
[14] M. Rontani, C. Cavazzoni, D. Bellucci, and G. Goldoni, J. Chem. Phys. **124**, 124102 (2006).
[15] A. Harju, H. Saarikoski and E. Räsänen, Phys. Rev. Lett. **96**, 126805 (2006).
[16] A. Ghosal, A. D. Güclü, C. J. Umrigar, D. Ullmo, and H. U. Baranger, Nat. Phys. **2**, 336 (2006).
[17] U. De Giovannini, F. Cavaliere, R. Cenni, M. Sassetti, and B. Kramer, New J. Phys. **9**, 93 (2007); U. De Giovannini, F. Cavaliere, R. Cenni, M. Sassetti and B. Kramer, Phys. Rev. B **77**, 035325 (2008); F. Cavaliere, U. De Giovannini, M. Sassetti, and B. Kramer, New J. Phys. **11**, 123004 (2009).
[18] A. Odriazola, A. Delgado, A. González, Phys. Rev. B **78**, 205320 (2008).
[19] A. Odriazola, J. Solanpää, I. Kylänpää, A. González, E. Räsänen, Phys. Rev. A **95**, 042511 (2017).
[20] J. Tiihonen, A. Schramm, I. Kylänpää, T. T. Rantala, J. Phys. D: Appl. Phys. **49**, 065103 (2016).
[21] I. Kylänpää, F. Berardi, E. Räsänen, P. Garcia-Gonzalez, C. Anrea Rossi, A. Rubio, New J. Phys. **18**, 083014 (2016).
[22] F. Cavaliere, N. Traverso Ziani, F. Negro, and M. Sassetti, J. Phys.: Condens. Matter **26**, 505301 (2014).
[23] D. M. Ceperley, Rev. Mod. Phys. **67**, 279 (1995).
[24] Ilkka Kylänpää and T. T. Rantala, J. Chem. Phys. **133**, 044312 (2010).
[25] I. Kylänpää and T. T. Rantala, J. Chem. Phys. **135**, 104310 (2011).
[26] I. Kylänpää, T. T. Rantala, and D. M. Ceperley, Phys. Rev. A **86**, 052506 (2012).
[27] D. M. Ceperley, J. Stat. Phys. **63**, 1237 (1991).
[28] R. P. Feynman "Statistical Mechanics" (Perseus Books, Reading, MA, 1998).
[29] N. Metropolis, A. W. Rosenbluth, M. N. Rosenbluth, A. H. Teller and E. Teller, J. Chem. Phys. **21**, 1087 (1953).
[30] C. Chakravarty, M. C. Gordillo and D. M. Ceperley, J. Chem. Phys. **109**, 2123 (1998).
[31] M.F. Herman, E. J. Bruskin, B. J. Berne, J. Chem. Phys. **76**, 5150 (1982).
[32] M. Taut, J. Phys. A **27**, 1045 (1994).